An improved expected temperature formula for identifying interplanetary coronal mass ejections

H. A. Elliott,[1] D. J. McComas,[1] N. A. Schwadron,[1] J. T. Gosling,[2] R. M. Skoug,[2] G. Gloeckler,[3] and T. H. Zurbuchen[4]

Received 17 September 2004; revised 25 November 2004; accepted 11 January 2005; published 16 April 2005.

[1] In this study we compare nearly 5 years of solar wind proton speed and temperature measurements from the Solar Wind Electron Proton Alpha Monitor (SWEPAM) on the Advanced Composition Explorer (ACE) to derive an improved expected temperature formula to identify interplanetary coronal mass ejections (ICMEs). Anomalously low proton temperatures have long been associated with ICMEs. When transient ICMEs are not present, the solar wind speed and temperature are highly correlated, and previous studies have derived fits to these measurements. Using these fits, an expected temperature is determined from the solar wind speed. Anomalously low temperatures have been identified as times when the ratio of the measured to expected temperature is below 0.5. In this study we remove ICMEs before fitting the remaining data. Fast and slow parcels in the solar wind interact and cause compressions and rarefactions as the solar wind moves away from the Sun. Since such interaction causes the speed and temperature of these parcels to change, we separately fit compression and rarefactions. We find that the expected temperature formula derived in this way provides a better way of identifying ICMEs than previous formulas, particularly in compression regions.

Citation: Elliott, H. A., D. J. McComas, N. A. Schwadron, J. T. Gosling, R. M. Skoug, G. Gloeckler, and T. H. Zurbuchen (2005), An improved expected temperature formula for identifying interplanetary coronal mass ejections, *J. Geophys. Res.*, *110*, A04103, doi:10.1029/2004JA010794.

1. Introduction

[2] Early in situ solar wind measurements showed that solar wind proton temperature and speed are generally well correlated [*Neugebauer and Snyder*, 1966]. Many studies since then have fit proton temperature (*Tp*) as a function of speed (*V*). The "expected temperature" (T_{ex}) is an estimate of the temperature determined from solar wind speed measurements using a formula based on a fit. One of the earliest fits was done by *Hundhausen et al.* [1970], who concluded that Vela 3 data could be fit well with either a linear fit to $\sqrt{Tp}$ or *Tp* versus *V*. *Burlaga and Ogilvie* [1970] fit $\sqrt{Tp}$ versus *V* in their analysis of Explorer 34 data. *Lopez and Freeman* [1986] found that the slope of the *Tp*-*V* curve changes at speeds >500 km s^{-1}, and they fit data above this value with either a line or a power law. Subsequent studies by *Lopez* [1987] and *Richardson and Cane* [1987] used linear fits at speeds >500 km s^{-1} and fit $\sqrt{Tp}$ versus *V* at speeds <500 km s^{-1}. *Neugebauer and Goldstein* [1997] used a single linear relationship between *V* and *Tp*. A more recent study by *Neugebauer et al.* [2003] used two separate quadratic fits at speeds above and below 450 km s^{-1}.

[3] By examining data over many years, *Burlaga and Ogilvie* [1973] and *Lopez and Freeman* [1986] found that the fits of *Tp* versus *V* do not vary significantly from year to year over the solar cycle. However, there are times when the proton temperature is anomalously low. *Gosling et al.* [1973] found such times tend to follow interplanetary shocks and to be associated with abnormally high He^{++}/H^{+} density ratios (>15%). They concluded that anomalously low proton temperatures were associated with expansion of solar ejecta (CMEs). Specifically, they mention that the low temperatures could be due to differing thermal properties caused by either disconnection of the ejecta from the Sun or from ejecta that stay connected to the Sun but originate from a small region on the Sun and then expand into large structures in solar wind.

[4] Interplanetary coronal mass ejections (ICMEs) can be identified using a variety of in situ measurements including magnetic field, solar wind ions, suprathermal electrons, energetic protons, heavy ion composition, and cosmic rays. Many ICMEs with high speeds are preceded by an interplanetary shock, and the ICMEs are often referred to as ejecta. Such shocks can be identified as sharp increases in speed, density, temperature, and field strength. Three long-established ICME (ejecta) criteria are low proton plasma beta ($\beta = n_p k T_p/(B^2/\mu_o)$), high n_α/n_p, and counterstreaming electrons which can indicate a closed magnetic field geometry

[1]Space Science and Engineering, Southwest Research Institute, San Antonio, Texas, USA.
[2]Los Alamos National Laboratory, Los Alamos, New Mexico, USA.
[3]Department of Physics, University of Maryland, College Park, Maryland, USA.
[4]Department of Atmospheric, Oceanic, and Space Science, University of Michigan, Ann Arbor, Michigan, USA.

0148-0227/05/2004JA010794

[e.g., *Gosling*, 1996, 1997; *Neugebauer and Goldstein*, 1997]. More recently, it has been established that large O^{7+}/O^{6+} density ratios (>1) are well associated with ICMEs, where such high O^{7+}/O^{6+} density ratios indicate ICMEs have higher than normal coronal temperatures [*Zurbuchen et al.*, 2002; *Henke et al.*, 2001]. *Gosling et al.* [1987] established the link between anomalously low temperature regions and ICMEs identified by the presence of counterstreaming electrons. They found that counterstreaming electron events had, on average, lower plasma betas, higher magnetic field strength, and lower proton and electron temperatures than surrounding solar wind. *Richardson and Cane* [1995] found $Tp/T_{ex} < 0.5$ to be a useful criterion for identifying ICMEs. Although many different ICME signatures are used to identify ICMEs, no one signature works all the time [e.g., *Gosling*, 1996; *Neugebauer and Goldstein*, 1997], and the presence of a given signature varies within an ICME [*Burlaga et al.*, 2001, and references therein]. Previous expected temperature studies (mentioned in the first paragraph) did not remove ICMEs prior to fitting *Tp* versus *V*. A unique aspect of our study is that we remove ICMEs using several criteria prior to fitting (section 2.2). We remove them because we seek an expected temperature formula that represents the relationship commonly found between *Tp* and *V* when ICMEs are not present.

[5] Not all missions have had extensive instrument suites, but most had a magnetometer and a bulk solar wind instrument. Therefore low Tp/T_{ex} was one of only a few ICME indicators available for some older missions (e.g., Voyager 1 and 2). An expected temperature formula played an important role in the recent Genesis mission, which was designed to determine the elemental and isotopic composition of the outer layers of the Sun by collecting samples in interplanetary space near 1 AU. Different collectors were exposed to the solar wind according to the type of wind being observed. Genesis had a sophisticated algorithm for determining the type of wind [*Neugebauer et al.*, 2003]. However, it did not have a magnetometer, so ICMEs were identified by several plasma properties: the presence of a shock, counterstreaming suprathermal electrons, high alpha to proton density ratios ($n\alpha/np$), and low Tp/T_{ex}. Since valid alpha particle and electron measurements are not always available, Tp/T_{ex} was at times an important criterion used to identify ICMEs.

[6] None of the previous studies treated compression and rarefaction regions separately. However, an early study by *Gosling et al.* [1972] modeled dynamic interactions and found that compressional heating could account for half the temperature rise observed on the leading edge of a high-speed stream. Later, *Gosling et al.* [1973] found that anomalously low proton temperatures were even lower than could be explained by rarefactional cooling in the trailing part of high-speed streams. *Lopez* [1987] and *Lopez and Freeman* [1986] estimated that stream-stream interactions would cause temperature variations between 12% and 22%. *Burlaga and Ogilvie* [1973] suggested that temperature could be separated into two components: one that depends on speed and another that depends on time. The time variation would represent the dynamic evolution of streams and the speed-dependent term would reflect the acceleration and heating near the Sun. Heating occurs in compressions as fast wind overtakes slow wind (increasing speed profile) and cooling occurs in rarefaction as fast wind outdistances slower trailing wind (decreasing speed profile). Since we expect compressions to be hotter and consequently to have a different *Tp-V* curve than rarefactions, we fit compressions and rarefactions separately (sections 2.3 and 2.4). Performing separate fits causes our formula to have higher T_{ex} in compressions and lower T_{ex} in rarefactions than previous formulas. *Gosling et al.* [1973] found anomalously low temperatures frequently occur when the speed profile is nearly constant or decreasing (rarefactions). We can determine if temperatures in compression regions associated with ICMEs are anomalously low relative to elevated temperatures typical for CIRs compressions.

2. Observations and Analysis

2.1. Instrumentation

[7] We use hourly averages of *V* and *Tp* determined from the Solar Wind Electron Proton Alpha Monitor (SWEPAM) [*McComas et al.*, 1998] on the Advanced Composition Explorer (ACE) spacecraft. Although SWEPAM ion measurements are available at 64 s resolution, we use the hourly ion measurements in our study since speed and temperature are well correlated on large scales. Consequently, our formulas as well as all other expected temperature formulas do not describe the small-scale structure associated with the shocks as discussed by *Ipavich et al.* [1998]. The *V* and *Tp* are derived from moments of proton distributions, and *Tp* is the radial proton temperature. To help identify and cull possible ICMEs, we also use hourly level 2 ACE magnetometer (MAG) measurements [*Smith et al.*, 1998] and ACE Solar Wind Ion Composition Spectrometer (SWICS) [*Gloeckler et al.*, 1998] heavy ion measurements. We analyze data starting from the first ACE SWEPAM measurements on day 035 of 1998 up through day 248 of 2003.

2.2. Culling ICMEs

[8] We identify ICMEs in the hourly data using three criteria: low proton plasma beta ($\beta < 0.1$), high alpha to proton density ratio ($n_\alpha/n_p > 0.8$), and high O^{7+} to O^{6+} density ratio ($n(O^{7+})/n(O^{6+}) > 1$). As mentioned in the introduction, low β and high $n\alpha/np$ are long-established ICME indicators [e.g., *Neugebauer and Goldstein*, 1997], and high $n(O^{7+})/n(O^{6+})$ recently has been established as a reliable ICME indicator [*Zurbuchen et al.*, 2002; *Henke et al.*, 2001]. Although this is not a comprehensive list of ICME signatures, the ones we selected are readily available and together provide reliable ICME identification. To ensure that we have excluded ICME times, we also remove any data points that fall within 24 hours of times when any one of our three criteria is satisfied.

[9] We use the above criteria to sort our data set into two primary groups: "possible" ICME data, satisfying any one of our ICME criteria or taken within a day of satisfying a criterion (Figure 1a), and "non-ICME" data remaining after removal of "possible" ICMEs (Figure 1c). We use only the "non-ICME" data to determine expected temperature formulas. Since the "likely" ICME category satisfies all three criteria, it is associated with the ejecta itself. However, since the "possible" ICME category corresponds to all data within 24 hours of a satisfied criterion, it includes the ejecta, some adjacent ambient solar wind, shocks, and

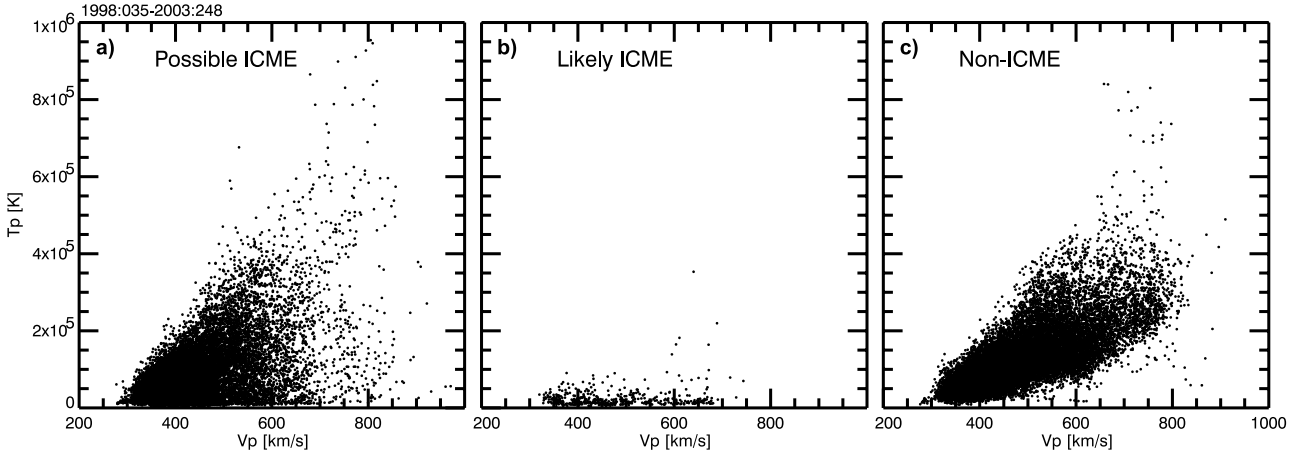

Figure 1. Solar wind proton temperature versus speed. (a) Data satisfying any of our criteria for being an ICME and data occurring within 24 hours of a satisfied criterion. (b) Data satisfying all three criteria. (c) Data remaining after culling ICMEs.

turbulent regions behind the shocks. In Figure 1b we show a subset of "possible" ICMEs called "likely" ICMEs, which satisfy all three criteria. These "likely" ICME data form a low-temperature branch off the main line of points, in part because beta is the ratio of thermal to magnetic pressure. Therefore low-proton beta can be caused by low temperatures. Our criteria are successful at removing most ICMEs from the "non-ICME" subset, although a small number may remain. As earlier studies have indicated *Tp* and *V* are well correlated for non-ICME data, and many ICMEs have low *Tp* and do not show a clear correlation between *Tp* and *V*.

2.3. Separating Compressions and Rarefactions

[10] After culling the data, we sort the data into compressions and rarefactions using the slope of a 2-day running average of solar wind speed versus time. Positive slopes are labeled as compressions, and negative slopes are labeled as rarefactions. However, if the magnitude of the slope is $<\pm 2.2 \times 10^{-4}$ km s^{-2}, it is labeled as "other." This slope criterion is large enough to remove times that are flat and small enough so that clear compressions and rarefactions are not categorized as "other." Figure 2 shows a solar wind speed time series separated into rarefactions (blue), compressions (orange), and "other" (black) regions. We apply this algorithm to the entire data set. Figure 3 shows the color-coded compressions and rarefactions with the ICMEs removed, and temperature is plotted on a logarithmic scale to clearly show the separation between compressions and rarefactions. As expected, the compression data is shifted to higher temperatures than the rarefaction data.

2.4. Fitting Compressions and Rarefactions Separately

[11] After sorting and culling the data, we analyze compression and rarefaction scatterplots of *Tp* versus *V* separately. The compressions and rarefactions are shown separately in Figure 4; it is clear that the solar wind at 1 AU (with ICMEs removed) rarely has speeds <300 km s^{-1} or >760 km s^{-1}. In addition to examining these scatterplots, we also placed the data with speeds between 300 km s^{-1} and 760 km s^{-1} data into 25 km s^{-1} speed bins and calculate average temperature for each bin (shown in black). We fit both the binned data and the individual hourly data points; we obtained similar formulas for both approaches. In Figure 4 we show the formulas for the fits to the binned data.

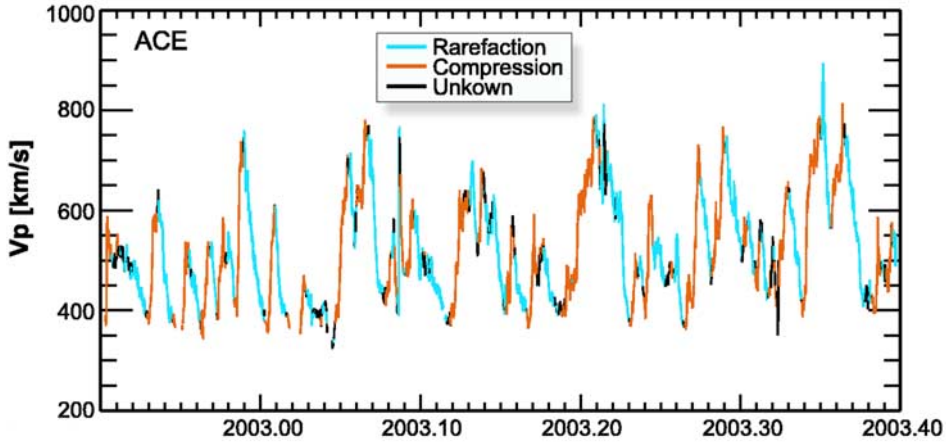

Figure 2. Solar wind speed time series separated into compressions (orange), rarefactions (bright blue), and "other" (black).

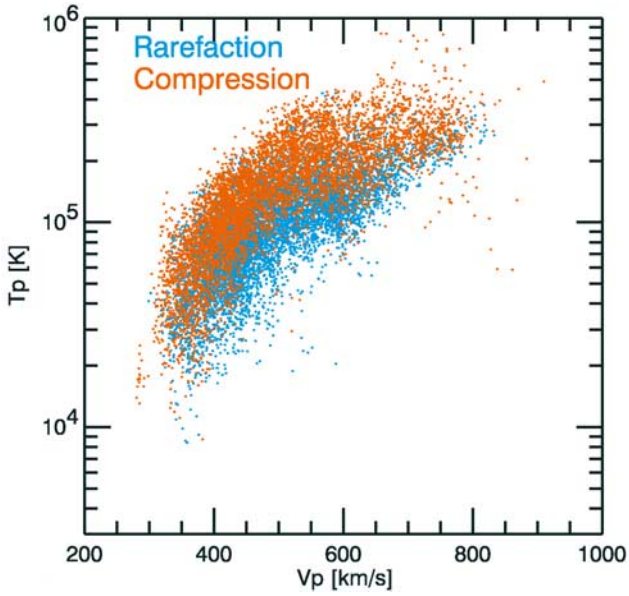

Figure 3. Temperature versus speed sorted into compressions (orange) and rarefactions (bright blue) after removing ICMEs. Temperature is on a logarithmic scale.

[12] We did not find the clear break in the 450–500 km s^{-1} range found in previous studies [*Lopez and Freeman*, 1986; *Lopez*, 1987; *Richardson and Cane*, 1987; *Neugebauer et al.*, 2003]. The rarefaction data have lower standard deviations and are well represented by a single line, but the compression data has larger standard deviations, particularly at high speeds (>575 km s^{-1}). The compression data is not as linear as the rarefactions, and at high speeds the compression data is so variable that we cannot determine definitively if there are two branches, a break at 575 km s^{-1}, or if the data is merely highly variable. More high-speed data is necessary to obtain a definitive answer, since a small number of events may skew the results. At high speeds the binned data seems to vary above and below the line, but given the high variability, a single line works well. Given the large standard deviations, many different functions could describe the high-speed data equally as well.

2.5. Assessing the Formula

[13] We assess how well our new formula works by comparing the measured with expected temperatures and by comparing our formula with the most recently published formula determined using ACE-SWEPAM measurements by *Neugebauer et al.* [2003, Figure 4]. From this point on we refer to this formula as the N2003 formula. Figure 5a shows the number of samples versus the ratio of the measured to expected temperature (Tp/T_{ex}) for the non-ICME data with compression in orange and rarefaction in blue. The Tp/T_{ex} distributions calculated using our new formulas are thick lines, and the N2003 distributions are thin. The two formulas have similar results in rarefaction regions except for a small difference in peak locations. The peak of the non-ICME rarefaction Tp/T_{ex} distributions for our formula and the N2003 one are both 0.83, reflecting the similarity between the rarefaction formulas. Much larger differences exist between the formulas in compression regions. The peak of the non-ICME compression Tp/T_{ex} distribution should ideally be centered on 1, but it is at 0.93 using our formula, and at 1.23 using the N2003 formula. We also determine what percentage of the non-ICME Tp/T_{ex} ratios lie within 15% of 1. In rarefactions that percentage is 33% for both formulas. However, in compressions the

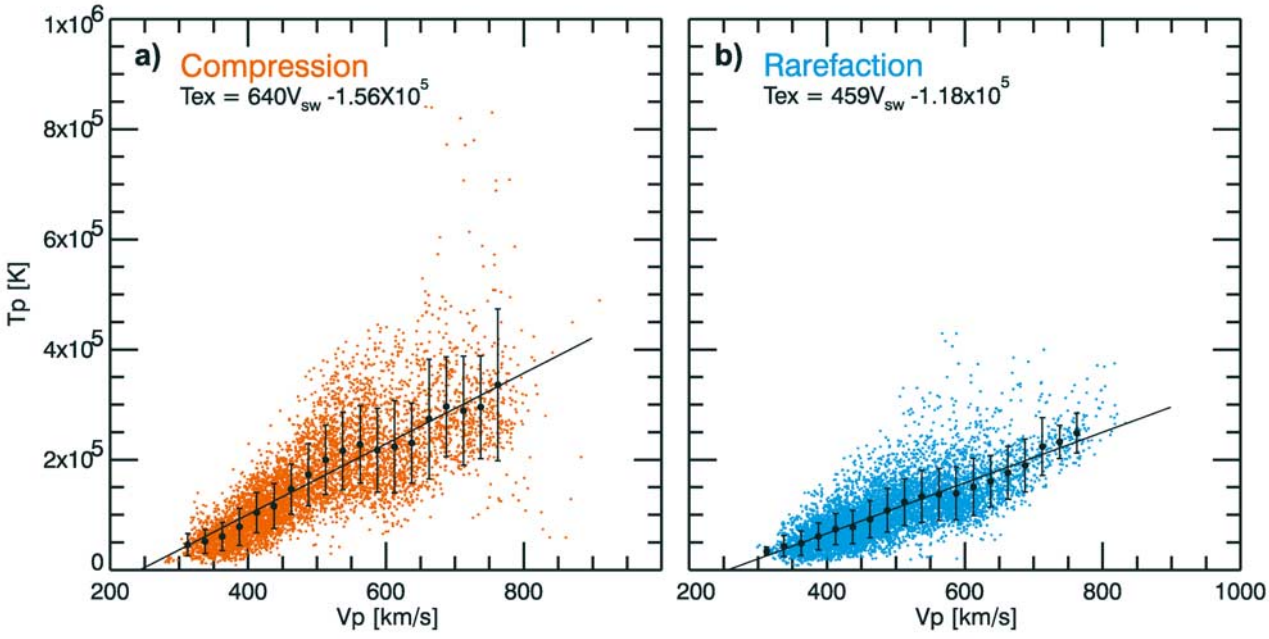

Figure 4. Linear fits to temperature versus speed where the compressions (left; orange) and rarefactions (right; bright blue) are fit separately. In black is average *Tp* for 25 km s^{-1} speed bins with the standard deviations shown as error bars. Only data with speeds between 300 km s^{-1} and 760 km s^{-1} are fit. The fit to the binned data is show as a solid black line.

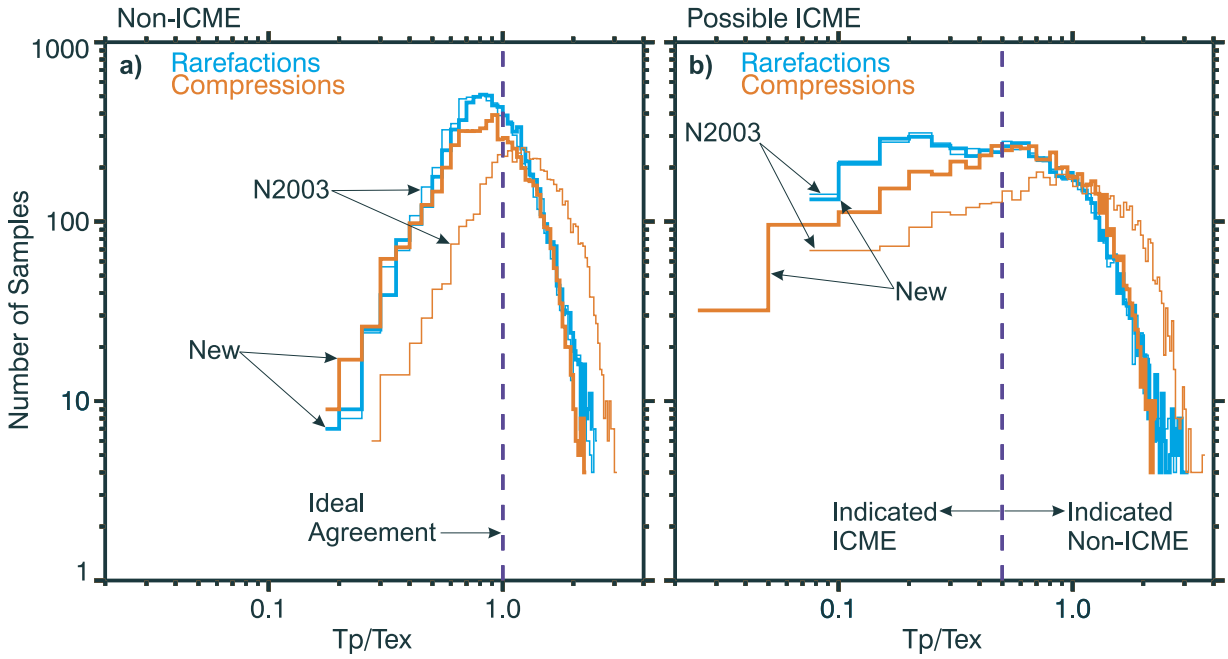

Figure 5. The number of samples with a given ratio of Tp/T_{ex} separately for (a) non-ICME data and (b) possible ICME data. Compressions are in orange and rarefactions in blue. The distributions for the N2003 formulas are thin lines and the distributions for our formulas are thick lines.

percentages for the two methods differ more, with our formula having 32% and the N2003 having 22%. Low proton temperatures are not exclusive to ICMEs, since some of the non-ICME data have low temperatures (Figure 5a). *Borrini et al.* [1981] and *Richardson and Cane* [1995] both found that low proton temperatures frequently occur near sector boundaries associated with the current sheet and surrounding plasma sheet.

[14] In Figure 5b we show the Tp/T_{ex} distributions for "possible" ICMEs. This plot shows that many ICMEs have low proton temperatures, and not all of the possible ICME data have low Tp/T_{ex}. The ICME rarefaction distributions are similar for the two methods, since the rarefaction formulas are similar. However, in compressions our new formula identifies more of the possible ICMEs than the N2003 formulas do. To further test the effectiveness of our formulas as a tool for identifying ICMEs, we determined what percentage of the "possible" and "likely" ICME data also had $Tp/T_{ex} < 0.5$ (Table 1). Both methods identify a higher percentage of the "likely" ICMEs. In rarefactions both methods identified the same percentages of likely and possible ICMEs. In compression regions our method identified 14% more of the "possible" ICME data (within a day of any satisfied criteria) and 8% more of the "likely" ICME data than the N2003 formula.

[15] Since we perform separate fits for compressions and rarefactions, our formulas always produce lower T_{ex} in rarefactions and higher T_{ex} in compressions than the N2003 formula. The advantage of performing separate fits is that differences between the expected and measured temperatures of the non-ICME data are reduced. Consequently, there will be a difference in the ICME identification if a fixed value of Tp/T_{ex} is used as a threshold criterion. We determined the percentage of ICME data with $Tp/T_{ex} < 0.5$ that is classified as compression, rarefaction, or other (Table 2). Using our formula, we find there is a higher percentage of this low Tp subset that are compressions than when we use the N2003 formula. Generally, more time is spent in rarefactions than in compressions, which leads to more data being collected in rarefactions than in compressions. The percentages of compression and rarefaction associated with anomalously low temperature ICMEs are nearly the same as the percentages as found in the ambient wind (Table 2).

3. Summary and Conclusions

[16] The majority of the data points meeting all three of the ICME criteria we have applied (low β, high n_α/n_p, high $n(O^{7+})/n(O^{6+})$) clearly have abnormally low proton temperatures. Low beta and high $n(O^{7+})/n(O^{6+})$ intervals are usually associated with magnetic clouds [*Henke et al.*, 2001; *Burlaga et al.*, 2001]. We did not look at additional magnetic cloud signatures, such as low variance in the field or rotations of the field. However, given that high $n(O^{7+})/n(O^{6+})$ intervals have been associated with magnetic clouds and that we find high $n(O^{7+})/n(O^{6+})$ intervals to have low ratios of Tp/T_{ex}, low Tp/T_{ex}, ratios might be a better indicator for magnetic clouds than other types of ICMEs.

[17] It is possible that removing ICME data using a more comprehensive list of ICME signatures might produce a more accurate formula, but we feel that our 24-hour criterion is strict enough to remove the majority of ICMEs

Table 1. Percentage of ICME Data Identified Using Each Formula

	Our Formula		N2003 Formula	
	Likely ICMEs	Possible ICMEs	Likely ICMEs	Possible ICMEs
Compressions	85%	29%	77%	15%
Rarefactions	83%	36%	83%	36%

Table 2. Percentage Data Identified as Compression, Rarefaction, or Other

		Possible ICMEs With Tp/T_{ex} <0.5	
	Ambient Wind	Our Formula	N2003 Formula
Compression	26%	28%	17%
Rarefaction	33%	37%	43%
Other	41%	35%	40%

from the data set. Our formulas do a better job of reproducing the measured temperatures of the non-ICME data. Furthermore, once we removed ICMEs and sorted the compressions and rarefactions, we did not find any clear break between 450 km s^{-1} and 500 km s^{-1} in the *Tp* versus *V* plots as reported in other studies [*Lopez and Freeman*, 1986; *Lopez*, 1987; *Richardson and Cane*, 1987; *Neugebauer et al.*, 2003]. Instead, we observed that at speeds greater than 600 km/s the standard deviation of the temperature increases. The break reported in other studies may reflect the separation between compressions and rarefactions, and the increased variability of the temperature at high speeds. Since no clear break was found, we fit one line covering the full range of speeds. Below are our formulas:

$$\text{Compressions}: \quad T_{ex} = 640V - 1.56 \times 10^5$$

$$\text{Rarefactions}: \quad T_{ex} = 459V - 1.18 \times 10^5.$$

This formula reproduces the large-scale linear trend between *V* and *Tp*. Since the data points are scattered about this curve, the formula does not reproduce small-scale structures.

[18] Compressions generally have higher proton temperatures than rarefactions, as shown in Figure 3, and our formulas reproduce this shift. Previous formulas fit all the data without sorting compressions and rarefactions, and the formula they obtained is closer to our rarefaction formula. Since our formulas produce expected temperatures closer to observed values, we can assess whether or not anomalously low *Tp* intervals tend to have increasing or decreasing speed profiles. Using our formulas, we find that 28% of the "possible" ICME data with anomalously low temperatures have an increasing speed profile (compression) and 37% have a decreasing profile (rarefaction). Since we compare ICME compressions to what is expected for non-ICME compressions, we find that ICME compressions are more anomalously low than previous formulas would indicate. However, the percentages of compression and rarefaction associated with anomalously low temperature ICMEs occurs with nearly the same as the percentages as in the ambient wind.

[19] Our expected temperature formulas identify more of the "possible" ICME data than the last published formula in compression regions, and in rarefaction regions both methods identify similar percentages. Our formulas provide expected temperatures that are closer to the measured temperatures and identify more data in the leading edges of ICMEs (compression regions) as anomalously low ($Tp/T_{ex} < 0.5$).

[20] **Acknowledgments.** We thank Lorna Wilson and Daveela Wilson for their work editing this paper and Pat Gonzales for graphic design work on the figures. This work was funded by NASA under the ACE-SWEPAM program.

[21] Shadia Rifai Habbal thanks Reinlad Kallenbach and Volker Bothmer for their assistance in evaluating this paper.

References

Borrini, G., J. M. Wilcox, J. T. Gosling, S. J. Bame, and W. C. Feldman (1981), Solar wind helium and hydrogen structure near the heliospheric current sheet—A signal of coronal streamers at 1 AU, *J. Geophys. Res.*, *86*, 4565.

Burlaga, L. F., and K. W. Ogilvie (1970), Heating of the solar wind, *Astrophys. J.*, *159*, 659.

Burlaga, L. F., and K. W. Ogilvie (1973), Solar wind temperature and speed, *J. Geophys. Res.*, *78*, 2028.

Burlaga, L. F., R. M. Skoug, C. W. Smith, D. F. Webb, T. H. Zurbuchen, and A. Reindard (2001), Fast ejecta during the ascending phase of the solar cycle 23: ACE observations, 1998–1999, *J. Geophys. Res.*, *106*, 20,957.

Gloeckler, G., et al. (1998), Investigation of the composition of solar and interstellar matter using solar wind and pickup ion measurements with SWICS and SWIMS on ACE, *Space Sci. Rev.*, *86*, 497.

Gosling, J. T. (1996), Corotating and transient solar wind flows in three dimensions, *Annu. Rev. Astron. Astrophys*, *34*, 35.

Gosling, J. T. (1997), Coronal mass ejections: An overview, in *Coronal Mass Ejections*, *Geophys. Monogr. Ser.*, vol. 99, edited by N. Crooker, J. A. Joselyn, and J. Feynman, p. 9, AGU, Washington, D. C.

Gosling, J. T., A. J. Hundhausen, V. Pizzo, and J. R. Asbridge (1972), Compressions and rarefactions in the solar wind: Vela 3, *J. Geophys. Res.*, *77*, 5442.

Gosling, J. T., V. Pizzo, and S. J. Bame (1973), Anomalously low proton temperatures in the solar wind following interplanetary shock waves—Evidence for magnetic bottles?, *J. Geophys. Res.*, *78*, 2001.

Gosling, J. T., D. N. Baker, S. J. Bame, W. C. Feldman, and R. D. Zwickl (1987), Bidirectional solar wind electron heat flux events, *J. Geophys. Res.*, *92*, 8519.

Henke, T., J. Woch, R. Schwenn, U. Mall, G. Gloeckler, R. von Steiger, R. J. Forsyth, and A. Balogh (2001), Ionization state and magnetic topology of coronal mass ejections, *J. Geophys. Res.*, *106*, 10,597.

Hundhausen, A. J., S. J. Bame, J. R. Asbridge, and S. J. Sydoriak (1970), Solar wind proton properties: Vela 3, observations from July 1965 to June, 1967, *J. Geophys. Res.*, *75*, 4643.

Ipavich, F. M., et al. (1998), Solar wind measurements with SOHO: The CELIAS/MTOF proton monitor, *J. Geophys. Res.*, *103*, 17,205.

Lopez, R. E. (1987), Solar cycle invariance in solar wind proton temperature relationships, *J. Geophys. Res.*, *92*, 11,189.

Lopez, R. E., and J. W. Freeman (1986), The solar wind proton temperature-velocity relationship, *J. Geophys. Res.*, *91*, 1701.

McComas, D. J., S. J. Bame, P. Barker, W. C. Feldman, J. L. Phillips, P. Riley, and J. W. Griffee (1998), Solar wind electron proton alpha monitor for the advanced composition explorer, *Space Sci. Rev.*, *86*, 563.

Neugebauer, M., and R. Goldstein (1997), Particle and field signatures of coronal mass ejections in the solar wind, in *Coronal Mass Ejections*, *Geophys. Monogr. Ser.*, vol. 99, edited by N. Crooker, J. A. Joselyn, and J. Feynman, p. 245, AGU, Washington, D. C.

Neugebauer, M., and C. W. Snyder (1966), Mariner 2 observations of the solar wind: 1. Average properties, *J. Geophys. Res.*, *71*, 4469.

Neugebauer, M., J. T. Steinberg, R. L. Tokar, B. L. Barraclough, E. E. Dors, R. C. Wiens, D. E. Gingerich, D. Luckey, and D. B. Whiteaker (2003), Genesis on-board determination of the solar wind flow regime, *Space Sci. Rev.*, *105*, 661.

Richardson, I. G., and H. V. Cane (1995), Regions of abnormally low proton temperature in the solar wind (1965–1991) and their association with ejecta, *J. Geophys. Res.*, *100*, 23,397.

Smith, C. W., J. L'Heureux, N. F. Ness, M. H. Acuna, L. F. Burlaga, and J. Scheifele (1998), The ACE magnetic fields experiment, *Space Sci. Rev.*, *86*, 613.

Zurbuchen, T. H., L. A. Fisk, G. Gloeckler, and R. von Steiger (2002), The solar wind composition throughout the solar cycle: A continuum of dynamic states, *Geophys. Res. Lett.*, *29*(9), 1352, doi:10.1029/2001GL013946.

H. A. Elliott, D. J. McComas, and N. A. Schwadron, Space Science and Engineering, Southwest Research Institute, P. O. Drawer 28510, San Antonio, TX 78228-0510, USA. (helliott@swri.edu)

G. Gloeckler, Department of Physics, University of Maryland, College Park, MD 20724, USA.

J. T. Gosling and R. M. Skoug, Los Alamos National Laboratory, Group ISR 1, MS D466, Los Alamos, NM 87545-0000, USA.

T. H. Zurbuchen, Department of Atmospheric, Oceanic, and Space Science, University of Michigan, 2455 Hayward Street, Ann Arbor, MI 48109, USA.